Original Article

JCBFM

Journal of Cerebral Blood Flow & Metabolism
2016, Vol. 36(6) 1143–1154

DOI: 10.1177/0271678X15606456
jcbfm.sagepub.com

SAGE

Detrimental role of pericyte Nox4 in the acute phase of brain ischemia

Ataru Nishimura[1,2], Tetsuro Ago[1,3], Junya Kuroda[1], Koichi Arimura[1,2], Masaki Tachibana[1], Kuniyuki Nakamura[1], Yoshinobu Wakisaka[1], Junichi Sadoshima[4], Koji Iihara[2] and Takanari Kitazono[1]

Abstract

Pericytes are mural cells abundantly present in cerebral microvessels and play important roles, including the formation and maintenance of the blood–brain barrier. Nox4 is a major source of reactive oxygen species in cardiovascular cells and modulate cellular functions, particularly under pathological conditions. In the present study, we found that the expression of Nox4 was markedly induced in microvascular cells, including pericytes, in peri-infarct areas after middle cerebral artery occlusion stroke models in mice. The upregulation of Nox4 was greater in a permanent middle cerebral artery occlusion model compared with an ischemia/reperfusion transient middle cerebral artery occlusion model. We performed permanent middle cerebral artery occlusion on mice with Nox4 overexpression in pericytes (Tg-Nox4). Infarct volume was significantly greater with enhanced reactive oxygen species production and blood–brain barrier breakdown in peri-infarct areas in Tg-Nox4, compared with littermate controls. In cultured brain pericytes, Nox4 was significantly upregulated by hypoxia and was promptly downregulated by reoxygenation. Phosphorylation of NFκB and production of matrix metalloproteinase 9 were significantly increased in both cultured pericytes overexpressing Nox4 and in peri-infarct areas in Tg-Nox4. Collectively, Nox4 is upregulated in pericytes in peri-infarct areas after acute brain ischemia and may enhance blood–brain barrier breakdown through activation of NFκB and matrix metalloproteinase 9, thereby causing enlargement of infarct volume.

Keywords

Brain ischemia, matrix metalloproteinase, NADPH oxidase, NFκB, pericytes

Received 8 February 2015; Revised 11 July 2015; Accepted 22 July 2015

Introduction

Recent evidence demonstrates that the structure and function of the neurovascular unit (a minimal unit to exert neuronal functions, consisting of neurons, astrocytes, endothelial cells, and pericytes) has to be protected to minimize neuronal damage after stroke.[1,2] Pericytes surround endothelial tubes with much higher coverage ratios in the brain than in other organs.[1,3] The higher coverage ratio of pericytes is closely associated with the specific presence of the blood–brain barrier (BBB), a tight junction formed by endothelial cells in the brain. Pericytes crucially regulate the stability of the BBB through the direct interaction with endothelial cells[3] and through the production of extracellular matrix proteins[4–6] and metalloproteinases (MMPs).[7] Dysfunction of pericytes directly leads to instability of the BBB and is involved in various disease states of the central nervous system (CNS), such as

[1]Department of Medicine and Clinical Science, Graduate School of Medical Sciences, Kyushu University, Fukuoka, Japan
[2]Department of Neurosurgery, Graduate School of Medical Sciences, Kyushu University, Fukuoka, Japan
[3]Innovation Center for Medical Redox Navigation, Graduate School of Medical Sciences, Kyushu University, Fukuoka, Japan
[4]Department of Cell Biology and Molecular Medicine, Cardiovascular Research Institute, Rutgers New Jersey Medical School, Newark, NJ, USA

Corresponding author:
Tetsuro Ago, Department of Medicine and Clinical Science, Graduate School of Medical Sciences, Kyushu University, 3-1-1 Maidashi, Higashi-ku, Fukuoka 812-8582, Japan.
Email: agou@intmed2.med.kyushu-u.ac.jp

stroke and Alzheimer disease.[8] Thus, much attention has been paid to pericytes in research of the CNS.

Reactive oxygen species (ROS) are important modulators of cellular functions in various cell types. It is thought that a large part of intracellular ROS is passively produced in the mitochondrial electron transport chain along with ATP generation under physiological conditions.[9] However, ROS are produced by enzymes other than mitochondrial enzymes, especially under pathological conditions.[10] Although there are many enzymes that can potentially produce ROS, the NADPH oxidase (Nox) family proteins are specialized to produce ROS in contrast to other ROS-producing enzymes.[10,11] Among five Nox family proteins (Nox1-5), it has been reported that Nox1, Nox2, and Nox4 can be expressed in cardiovascular cells.[12,13] Nox2 is the prototypical Nox expressed mainly in phagocytic cells and can produce a burst of ROS by forming a complex with the specific cytosolic proteins in a stimulus-dependent manner to play a bactericidal role.[11] Nox1 is expressed in smooth muscle cells[14] and may be involved in the development of hypertension and atherosclerosis.[15] Nox4 is expressed ubiquitously with higher expression in cardiovascular cells, such as endothelial cells,[16–18] smooth muscle cells (SMCs),[19] and cardiac myocytes.[20–22] Nox4 is a unique enzyme because it can constitutively produce smaller amounts of ROS without cytosolic activators in contrast to other Nox proteins.[10–12] It is thought that the amount of ROS produced by Nox4 correlates well with its expression levels in cells.[23,24]

In this study, we found that Nox4 was expressed in cerebral microvascular pericytes in the intact brain and its expression was markedly upregulated in peri-infarct areas after acute brain ischemia. We therefore investigated the roles of pericyte Nox4 in acute brain ischemia, using both mice and cultured brain pericytes that overexpressed Nox4.

Materials and methods

Animals

All animal experiments were conducted according to the Guidelines for Proper Conduct of Animal Experiments by the Science Council of Japan (1 Jun 2006) (http://www.scj.go.jp/ja/info/kohyo/pdf/kohyo-20-k16-2e.pdf). All animal procedures were approved by the Animal Care and Use Review Committee of Kyushu University (Fukuoka, Japan) (A25-268-1). We used a total of 104 FVB/N wild-type (WT) male mice aged 8–13 weeks weighing 20–35 g and 86 FVB/N male mice with the same ages and weights overexpressing human Nox4 in vascular mural cells driven by SM22α promoter (Tg-Nox4), which were originally generated in Prof. Junichi Sadoshima's laboratory (Rutgers New Jersey Medical School, NJ, USA). It is known that transgenic mice can be generated more easily in FVB/N than in C57BL/6.[25] Mice were reproduced and housed two per cage in the animal facility of Kyushu University at 21°C and 65% humidity with a regulated 12-hour light–dark cycle and with free access to food and water. Mice were randomly assigned to the operator, and independent persons not involved in animal procedures analyzed parameters. The mice number used for each experiment is summarized in Supplementary Table 1. We performed each experiment group independently to avoid "nesting". The following conditions excluded mice from analyses: (1) death within 24 hours after MCAO (WT (n = 4) and Tg-Nox4 (n = 9)), (2) subarachnoid hemorrhage or bleeding into the brain parenchyma (WT (n = 2) and Tg-Nox4 (n = 5)), and (3) operation time >40 minutes (WT (n = 1) and Tg-Nox4 (n = 2)). Experiments were reported according to the ARRIVE guidelines.

Stroke models

Focal brain ischemia was produced using two different methods, pMCAO[26,27] or tMCAO,[28] as described previously. Cerebral blood flow before and during ischemia was measured at the ipsilateral parietal bone (2 mm posterior and 5 mm lateral to bregma) using the laser Doppler flowmeter (PeriFlux System 5000, PERIMED, Stockholm, Sweden). Operated mice were sacrificed with deep anesthesia using intraperitoneal administration of pentobarbital (150 mg/kg body weight) at the indicated day after MCAO and were perfused transcardially with ice-cold heparinized saline and 4% paraformaldehyde. The brains were quickly removed, and fresh coronal sections (2 mm thick) were fixed with 4% paraformaldehyde in phosphate-buffered saline (PBS) for immunohistochemistry. Infarct volume was measured by indirect method with staining with 2% 2,3,5-triphenyltetrazolium chloride (TTC) in each section: infarct volume (mm^3) = summation of each slice [{(contralateral total area (mm^2)) – (ipsilateral non-infarct area (mm^2))} × 2 mm (thick)].[29]

Immunohistochemistry and immunofluorescence

Paraformaldehyde-fixed coronal sections were embedded in optimum cutting temperature compound and were cut into 20-μm-thick slices. Sections were blocked with PBS containing 5% normal goat serum for 1 hour at room temperature. Next, sections were incubated with primary antibodies [Nox4 (Abcam # 60940, 1:100 dilution), PDGFRβ (Cell Signaling Technology (CST) (Boston, MA, USA) # 3169, 1:50 dilution), SM22α (Abcam # 28811, 1:50 dilution),

NeuN (Millipore # 377, 1:100 dilution)], or fluorescein 5′-isothiocynate (FITC)-lectin overnight at 4°C. Secondary antibodies (affinity-purified anti-rabbit or mouse immunoglobulin G; Nichirei Corporation, Japan) were incubated for 30 minutes at room temperature. The slides were observed using Z-stack function (2-μm intervals) on a BIOREVO BZ-9000 fluorescence microscope (Keyence, Japan).

Assessment of BBB breakdown

Permeability of the BBB in infarct areas was assessed by the leakage of FITC-dextran (MW 70 kDa, Sigma-Aldrich, 0.5 mL of a 2% solution in saline) or Evans blue dye (Sigma-Aldrich, 0.1 mL of a 2% solution in saline).[30] Briefly, the brain was collected 120 minutes after the FITC-dextran or Evans blue dye was injected intravenously via the tail vein. For the leakage of FITC-dextran, fluorescence intensity of five regions of interest (ROI: 100 μm × 100 μm) in FITC-dextran-leaked peri-infarct areas and in the contralateral non-ischemic regions was measured using the BZ-II analyzer software (Keyence).

Assessment of capillary density

Capillaries were labeled with FITC-lectin injected from jugular vein 30 minutes before sacrifice. Capillary density was measured using the ImageJ to determine pixel number per image. A total of three ROI (500 × 500 μm) in the peri-infarct area of parietal cortex and the lateral striatum were evaluated. Fold change of capillary density was calculated as compared with that in the contralateral non-ischemic areas.

Gelatin zymography

Isolated brain was homogenized with lysis buffer (50 mmol/L Tris-HCl (pH 7.4), 150 mmol/L NaCl, 5 mmol/L $CaCl_2$, 0.05% Brij-35, and 1% Triton X-100). The homogenates were incubated overnight with gelatin-sepharose beads (Gelatin Sepharose 4B; GE Healthcare) at 4°C. After incubation and centrifugation, samples were resuspended for 2 hours in 200 μL of elution buffer containing dimethyl sulfoxide. The samples were applied to the Gelatin-Zymography Kit (Cosmobio Co., Ltd., Japan) according to the manufacturer's instructions. Briefly, the samples were separated on gelatin gel, and the gel was soaked in washing buffer for 1 hour at room temperature followed by a 24-hour incubation at 37°C in reaction buffer. To visualize the activity of MMPs, the gel was stained with staining solution for 30 minutes. Relative gelatinase activity against MMP-9 and MMP-2 standard was quantified by measuring optical density using the ImageJ.

Cell culture

Human brain microvascular pericytes and SMCs isolated from normal adult tissues were purchased from Cell Systems (Kirkland, WA, USA).[26] The cells were plated on collagen type I-coated dishes (Iwaki Glass, Japan) and cultured with the CS-C medium kit (Cell Systems) supplemented with 10% fetal bovine serum. The cells were cultured at 37°C in 5% CO_2 in a humidified incubator. Cells at passage 3 to 5 were used for experiments. Nox4 inhibitors, VAS2870 (Enzo Life Science, Japan) and GKT137831 (Genkyotex S.A., Switzerland), were used to test their effects to MMP-9 activity in cultured pericytes.

Adenoviruses

Adenovirus harboring Nox4 (Ad-Nox4) or LacZ (Ad-LacZ, as a control) was generated using the AdMax system (Clontech Laboratories, Inc., Mountain View, CA, USA) as described previously.[20] The adenoviruses were amplified in HEK293 cells.

Reverse transcription-PCR and real-time PCR

Preparation of total RNA from cultured cells or brain tissues, reverse-transcription, polymerase chain reaction (PCR), and quantitative real-time PCR were performed as described previously.[26] One microgram of total RNA was reverse-transcribed in a total volume of 20 μL, and 0.5 μL of the product was used as a template. The mRNA copy numbers were standardized using 18 s ribosomal RNA (18 s rRNA). Primers used in the present study are listed in Supplementary Table 2.

Immunoblot analyses

Immunoblot analyses using brain homogenates or cell lysates were performed as described previously.[26] Primary antibodies were purchased from CST [total NFκB (# 8482, 1:1000 dilution), phospho-NFκB (# 3033, 1:1000 dilution), IκB (# 4814, 1:1000 dilution), IKKα (# 11930, 1:1000 dilution), IKKβ (# 8943, 1:1000 dilution), phospho-IKKαβ (# 2697, 1:1000 dilution)], and Sigma-Aldrich (St. Louis, MO, USA) [β-actin (AS441, 1:4000 dilution)].

Statistical analysis

All values are expressed as means ± SD. Statistical analyses between groups were performed by unpaired Student's t test or one-way analysis of variance followed by a Bonferroni post hoc test. A value of $p < 0.05$ was regarded as statistically significant.

Results

Temporal and spatial expression profiles of Nox4 in acute ischemic stroke models

We first examined Nox4 expression in the intact mouse brain. Double immunofluorescent staining demonstrated that Nox4 could be identified in lectin-positive endothelial cells, PDGFRβ−positive mural cells of small vessels, and NeuN-positive neurons in the intact brain at higher magnifications, although their expression levels were all very low (Figure 1a). We applied two different stroke models, pMCAO and tMCAO, and examined temporal and spatial expression of Nox4 in the brain. Quantitative PCR using total RNA prepared from brain homogenates showed that Nox4 was significantly upregulated in the ischemic hemisphere from day 1 to 7 with the maximum level seen at day 4 after pMCAO by 28.9-fold (Figure 1b, left). Consistently, immunofluorescent staining demonstrated that Nox4 expression was markedly upregulated in peri-infarct areas after pMCAO (Figure 1c, middle) with the maximum level observed at day 4 (Supplementary Figure 1a), although it was very marginal at baseline at a low magnification (Figure 1c left). In comparison, the upregulation of Nox4 was also found in ischemic areas after tMCAO with the similar temporal profile with that of pMCAO (Figure 1b, right) but was lower in tMCAO (by 9.3-fold at day 4) than in pMCAO (Figure 1b and c). Immunofluorescent double labeling demonstrated that the upregulated Nox4 was labeled with cells expressing lectin (Figure 1d, top), and strongly with cells expressing PDGFRβ, a pericyte marker in microvessels[31] (Figure 1d, middle), in peri-infarct areas after pMCAO. The expression of neuronal Nox4 did not appear to increase after pMCAO, although the number of survival neurons was small in the areas where Nox4 was highly upregulated (Figure 1d, bottom). The expression pattern of Nox4 after tMCAO was basically same to that of pMCAO except that the extent of Nox4 upregulation in vascular cells was markedly lower (Supplementary Figure 1b).

Infarct volume and BBB breakdown increases in Tg-Nox4 animals

To determine the effects of upregulated Nox4 in vascular mural pericytes in peri-infarct areas, we used mice overexpressing *human* Nox4 in pericytes using an SM22α-promoter region (Tg-Nox4). We confirmed by immunofluorescent double labeling that SM22α was expressed in PDGFRβ-positive pericytes in peri-infarct areas (Supplementary Figure 2a). Furthermore, using human-specific primers for Nox4, we confirmed that *human* Nox4 transgene was expressed in microvessels isolated from the transgenic mouse brain (Supplementary Figure 2b). Tg-Nox4 mice had apparently normal physiological parameters, including body weight, blood pressure, heart rate, and cerebral blood flow, with normal cerebrovascular structure, compared with those of littermate WT controls (Supplementary Table 3).

We performed pMCAO on Tg-Nox4 mice. Reduction of cerebral blood flow during pMCAO was not significantly different between WT and Tg-Nox4 (Supplementary Figure 3a). TTC staining demonstrated that infarct volume at day 4 was significantly larger in the transgenic mice ($44.0 \pm 4.1\,mm^3$, $n = 11$) than in WT mice ($33.5 \pm 3.5\,mm^3$, $n = 10$) (Figure 2a). Immunofluorescent staining showed that Nox4 expression (Figure 2b) and ROS production in vascular cells (Supplementary Figure 3b (arrows)) in peri-infarct areas were greater in Tg-Nox4 than in WT mice. We confirmed by immunofluorescence that the increase in post-stroke upregulation of Nox4 was specific for pericytes in Tg-Nox4 (Supplementary Figure 3c). We next examined BBB breakdown in ischemic areas at day 4 after pMCAO. The extravasation of Evans blue dye, particularly in peri-infarct areas where Nox4 was upregulated, was greater in Tg-Nox4 than in WT (Figure 2c). Consistently, BBB breakdown assessed by the leakage of FITC-dextran (70 kDa) was also significantly greater in Tg-Nox4 than in WT (Figure 2d). In contrast, capillary density as assessed by FITC-lectin in peri-infarct area at day 4 was not significantly different between WT and Tg-Nox4 (Figure 2e). Collectively, increased expression of Nox4 in microvascular pericytes in peri-infarct areas was associated with the enhanced BBB breakdown in acute brain ischemia, thereby causing the enlargement of infarct volume.

Nox4 is upregulated by hypoxia and is downregulated by reoxygenation in cultured brain pericytes

We next investigated the mechanisms by which Nox4 was more greatly upregulated in pericytes rather than larger vessel SMCs in peri-infarct areas during brain ischemia, using cultured cells. We confirmed that brain pericytes specifically expressed Nox4 among the Nox family proteins, although SMCs expressed Nox4 along with Nox1, as reported previously (Figure 3a).[19,32] Quantitative PCR using the same amount of total RNA demonstrated that the expression level of Nox4 at baseline was significantly higher in pericytes than in SMCs (Figure 3b). We examined the effects of hypoxia and hypoxia/reoxygenation on the expression of Nox4 in these cultured cells. Hypoxia at 1% O_2 for over 24 hours significantly upregulated the expression of Nox4 in both cell types (Figure 3b). However, the increase was more prominent in pericytes (Figure 3b). Reoxygenation after hypoxia promptly downregulated

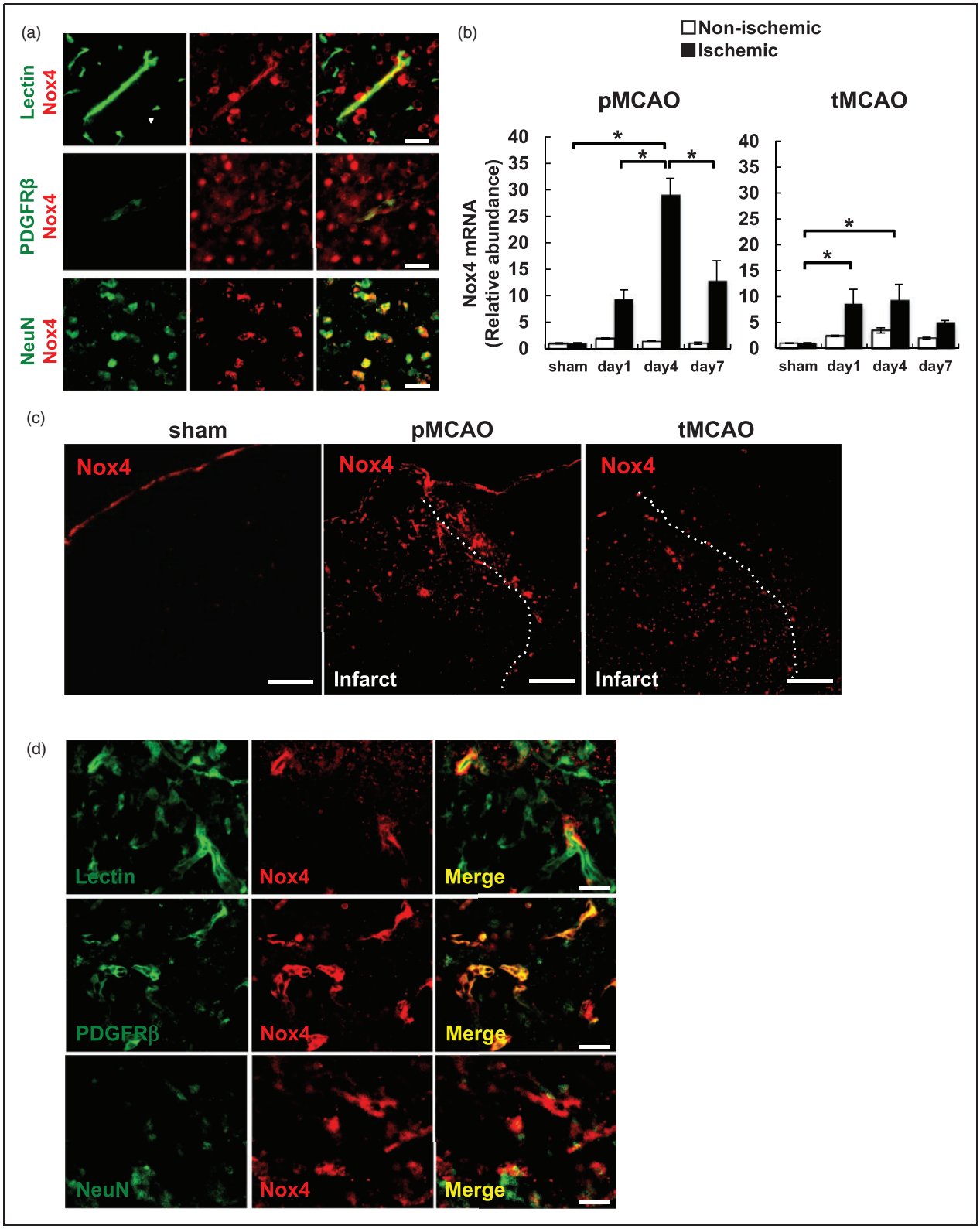

Figure 1. Expression of Nox4 in ischemic areas after pMCAO and tMCAO stroke models. (a) Immunofluorescent double staining of Nox4 (red) and lectin (green), an endothelial cell marker (top), PDGFRβ (green), a pericyte marker (middle), or NeuN (green), a neuronal marker (bottom) in the intact mouse brain (scale bar: 20 μm). (b) The expression changes of Nox4 mRNA in non-ischemic and ischemic hemisphere at day 1, 4, and 7 after pMCAO (b, left) and tMCAO (b, right) was examined by quantitative real-time PCR. Values are mean ± SD ($n = 4$ for each time point, $^*p < 0.05$). (c) Immunofluorescent staining of Nox4 at a low magnification in the hemisphere of sham-operated mice (left), and in peri-infarct areas at day 4 after pMCAO (middle) or tMCAO (right) (scale bar: 500 μm). (d) Immunofluorescent double staining of Nox4 (red) and lectin (green) (top), PDGFRβ (green) (middle), or NeuN (green) (bottom) in peri-infarct area at day 4 after pMCAO (scale bar: 20 μm).

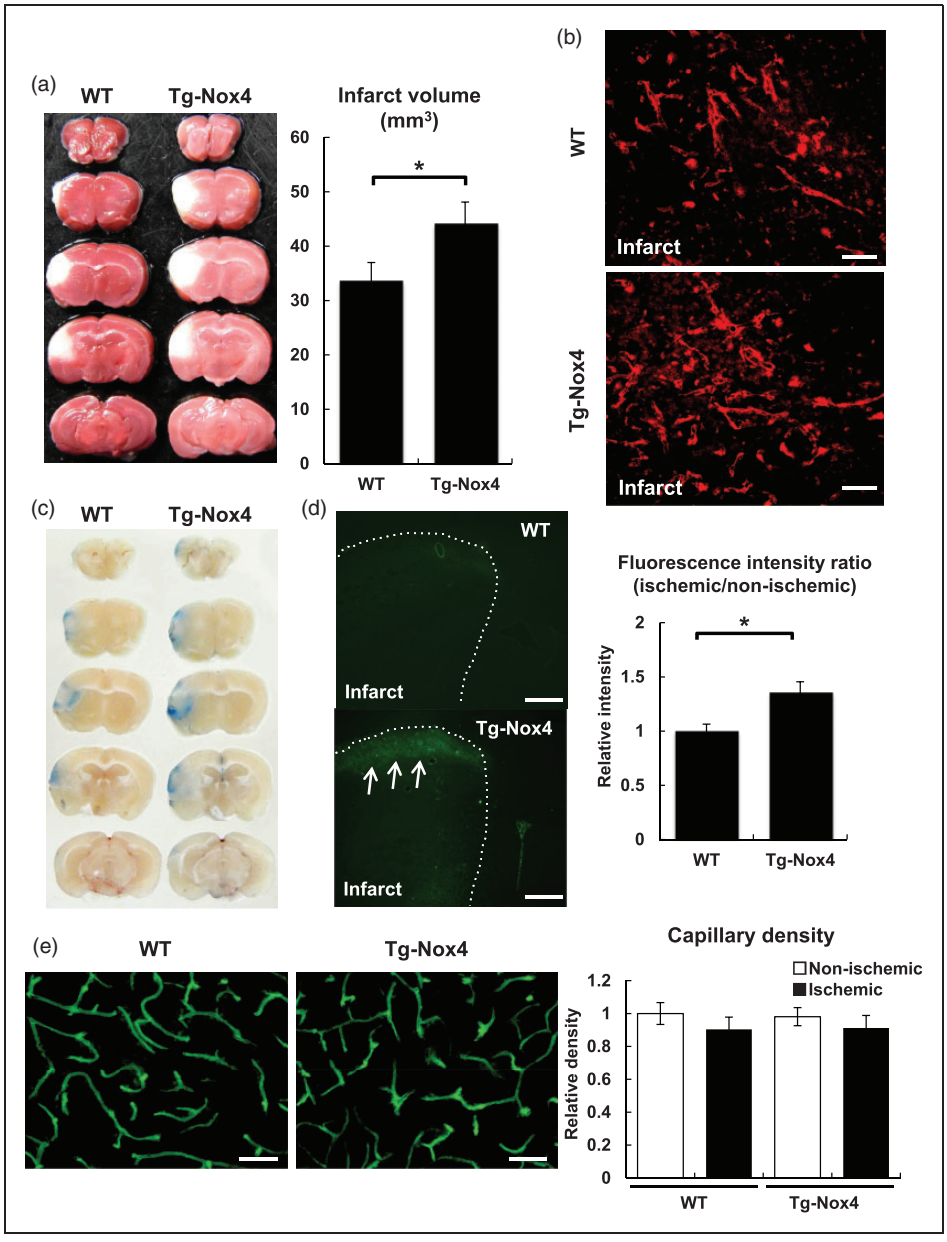

Figure 2. Phenotypic changes of Tg-Nox4 in pMCAO. (a) Infarct volume at day 4 after pMCAO was measured by TTC staining in WT (left) and Tg-Nox4 (right). Representative TTC stains are shown. Values are mean ± SD (WT (n = 10) and Tg-Nox4 (n = 11), $^*p < 0.05$). (b) Representative immunofluorescent staining of Nox4 in peri-infarct areas at day 4 after pMCAO in WT (top) and Tg-Nox4 (bottom) (scale bar: 50 μm). BBB breakdown was assessed by the leakage of Evans blue dye (c) or FITC-dextran (70 kDa) in ischemic areas at day 4 after pMCAO in WT (d, top) and Tg-Nox4 (d, bottom, arrows) (scale bar: 500 μm). Values are mean ± SD (WT (n = 11) and Tg-Nox4 (n = 11), $^*p < 0.05$) (d, right). (e) Capillary density in peri-infarct areas at day 4 after pMCAO in WT (left) and Tg-Nox4 (right) (scale bar: 50 μm). Values are mean ± SD (WT (n = 6) and Tg-Nox4 (n = 6), $^*p < 0.05$).

Nox4 expression to basal levels within 24 hours in cultured pericytes (Figure 3c).

Molecular mechanisms by which pericyte Nox4 enhances BBB breakdown

To elucidate the molecular mechanisms underlying Nox4-mediated enhancement of BBB breakdown in vivo, we induced adenovirus-mediated Nox4 overexpression in cultured brain pericytes (Figure 4a). We found that the expression of metalloproteinase-9 (MMP-9), a key molecule participating in BBB breakdown, was significantly upregulated in Nox4-overexpressing pericytes, whereas another major gelatinase MMP-2 was not significantly upregulated in the cells (Figure 4b). Using gelatin zymography of culture media, we found

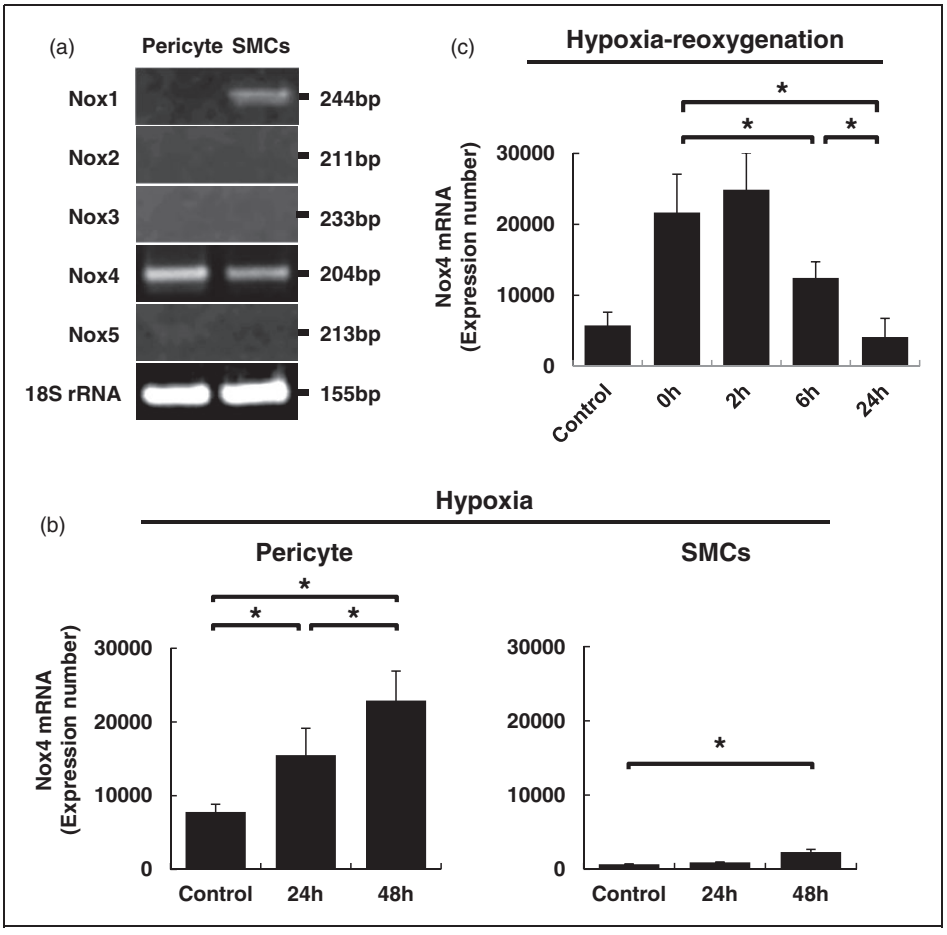

Figure 3. Expression of the Nox family proteins in cultured vascular mural cells. (a) PCR analysis of the Nox family proteins and 18 s rRNA in cultured brain microvascular pericytes and SMCs. (b) Relative gene expression of Nox4 mRNA at baseline and at 1% hypoxia for 24 and 48 hours in cultured pericytes and SMCs. Values are mean ± SD ($n = 3$, $^*p < 0.05$). (c) Effects of reoxygenation for 0, 2, 6, and 24 hours on the hypoxia-induced Nox4 upregulation. Values are mean ± SD ($n = 3$, $^*p < 0.05$).

that greater amounts of enzymatically active MMP-9 were secreted into culture media in Nox4-overexpressing pericytes compared with Lac Z-overexpressing pericytes (Figure 4c). In contrast, the treatment of cultured pericytes with a Nox4 inhibitor, VAS2870 (10 μM) or GKT137831 (10 μM), attenuated MMP-9 activity in culture media (Supplementary Figure 4).

We also investigated upstream molecules that could increase the expression of MMP-9. Among the possible transcription factors we tested, we found a significant increase in the phosphorylation of NFκB (Figure 4d), along with increases in the phosphorylation of IκB kinase complex (IKKαβ) and IκB degradation (Figure 4e), in cultured pericytes overexpressing Nox4.

NFκB–MMP-9 signaling increases in peri-infarct areas after pMCAO in Tg-Nox4

Finally, we examined whether the activation of NFκB and the increased production of MMP-9 were found in peri-infarct areas at day 4 after pMCAO in Tg-Nox4. Gelatin zymography using brain homogenates demonstrated that the metalloproteinase activity of MMP-9, along with MMP-2, was significantly increased in the ischemic hemisphere, compared with the non-ischemic one, in both WT mice and Tg-Nox4 (Figure 5a). The increase in MMP-9 activity, but not in MMP-2 activity, was significantly greater in Tg-Nox4 than in WT (Figure 5a). In parallel with the increase in MMP-9 activity, greater amounts of NFκB phosphorylation were found in the ischemic hemisphere of Tg-Nox4 than in that of WT (Figure 5b).

Discussion

In the present study, we have demonstrated that the expression of Nox4 is remarkably upregulated in microvascular pericytes in peri-infarct areas after MCAO, and the upregulated Nox4 increases the production of MMP-9 probably through NFκB in pericytes and can

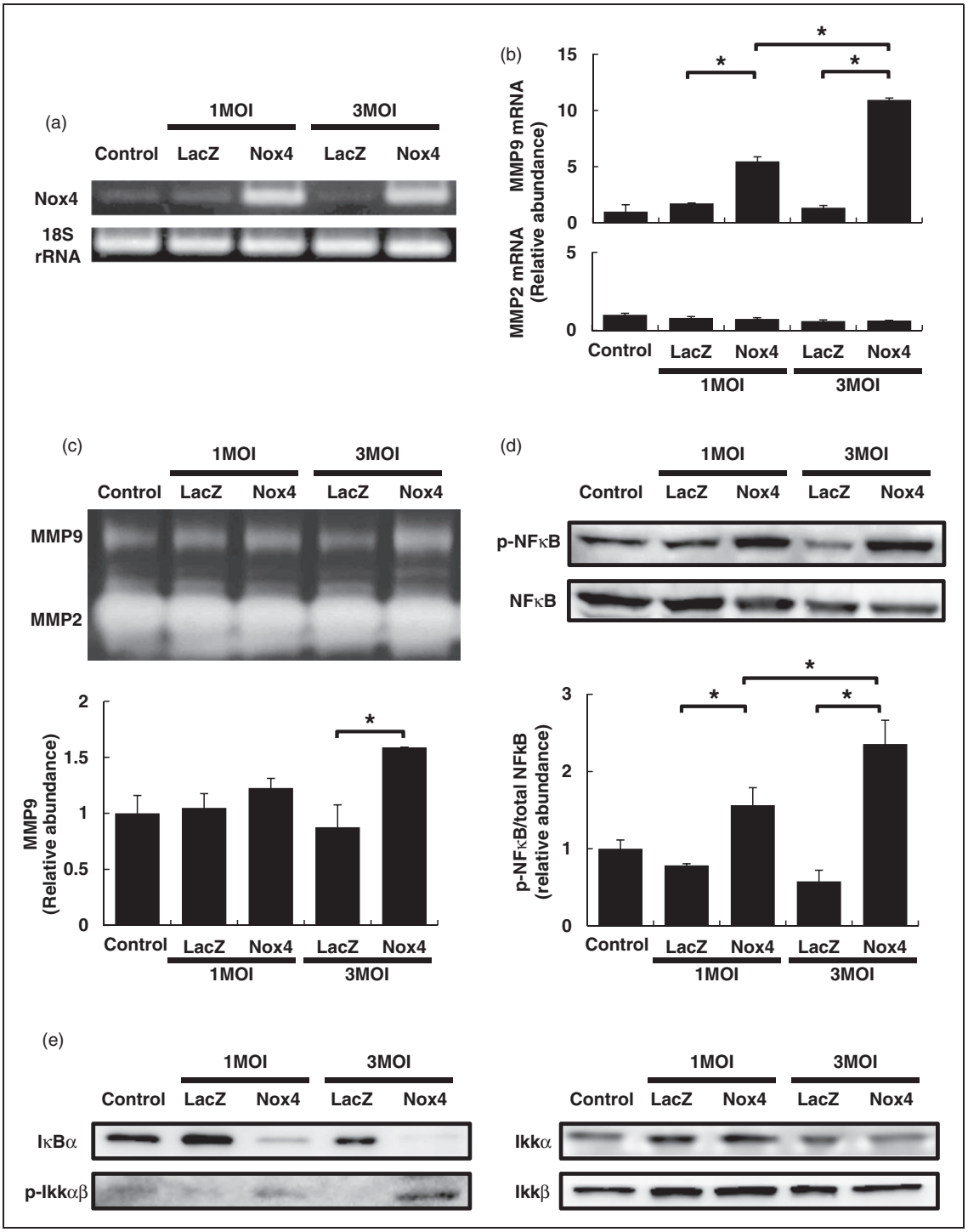

Figure 4. Mechanisms underlying pericyte Nox4-mediated enhancement of BBB breakdown. (a) Confirmation of adenovirus-mediated Nox4 overexpression in cultured pericytes. (b) Expression changes of two gelatinases, MMP-9 and MMP-2, in cultured pericytes overexpressing LacZ or Nox4. Values are mean ± SD (n = 3, $^*p < 0.05$). (c) Gelatin zymography using media from cultured pericytes overexpressing LacZ or Nox4. Values are mean ± SD (n = 3, $^*p < 0.05$). (d) Immunoblot analyses of NFκB and phospho-NFκB in pericytes overexpressing LacZ or Nox4. Values (= ratios of phospho-NFκB to total NFκB) are mean ± SD (n = 3, $^*p < 0.05$). (e) Representative immunoblot analyses of IκB, IKKα, IKKβ, and phospho-IKKαβ in pericytes overexpressing LacZ or Nox4 (n = 3).

deteriorate BBB breakdown, thereby causing the enlargement of infarct volume. This is the first report demonstrating the effects of Nox4 upregulated in microvascular pericytes during acute brain ischemia.

Brain pericytes express Nox4

We showed that brain pericytes specifically expressed Nox4 among the Nox family proteins (Figure 3), and its expression level was significantly increased under hypoxic conditions both in vivo (Figure 1) and in vitro (Figure 3). Pericytes and SMCs are both mesenchyme-derived vascular mural cells that have similar cellular functions and protein expression profiles. Although both cells expressed Nox4, its expression level was much higher at baseline and was more strongly induced by hypoxia in pericytes than in SMCs (Figure 3). Consistent with the findings in vitro, the expression of Nox4, as assessed by immunofluorescence, was induced more prominently in microvascular pericytes than in SMCs in peri-infarct areas after MCAO (Figure 1c and d). Because more peripheral microvascular pericytes are exposed to lower oxygen tension than SMCs,[33] pericytes may be able to express higher amounts of Nox4 than SMCs, particularly under ischemic conditions in vivo. This expression pattern was maintained in Tg-Nox4 (Figure 2b and Supplementary Figure 3c).

We also found that the expression of Nox4 was increased in lectin-positive endothelial cells in peri-infarct areas after brain ischemia (Figure 1d). We have reported previously that Nox4 is a major ROS-producing enzyme in endothelial cells[16] and thus consider that endothelial Nox4 should also play an important role after brain ischemia. We actually examined the roles of endothelial Nox4 after MCAO, using the mice with endothelial cell-specific Nox4 overexpression. Endothelial Nox4 appears to function

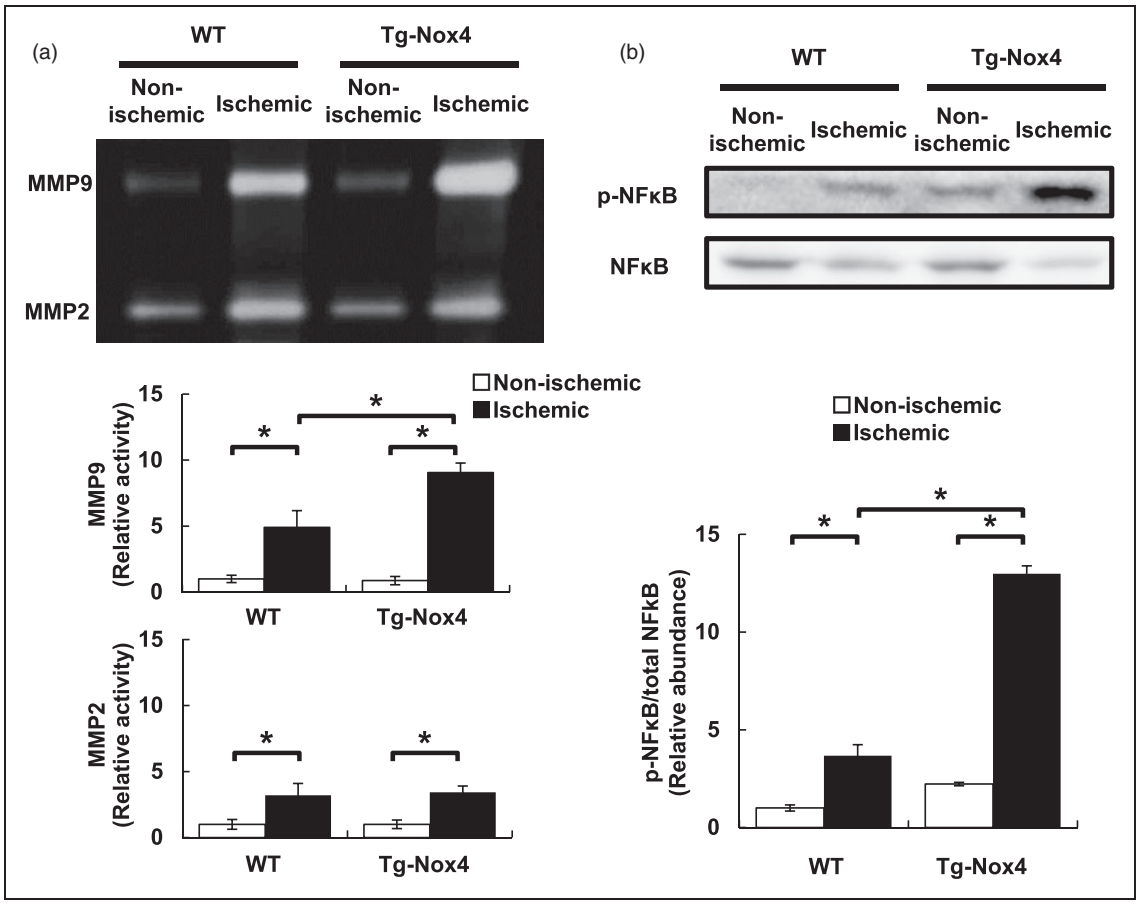

Figure 5. Increased phosphorylation of NFκB and production of MMP-9 in peri-infarct areas at day 4 after pMCAO in Tg-Nox4. (a) Gelatin zymography using homogenates prepared from non-ischemic and ischemic hemispheres at day 4 after pMCAO in WT and Tg-Nox4. Values are mean ± SD (WT (n = 6) and Tg-Nox4 (n = 6), $*p < 0.05$). (b) Immunoblot analyses of NFκB and phospho-NFκB using homogenates prepared from non-ischemic and ischemic hemispheres in WT and Tg-Nox4. Values are mean ± SD (WT (n = 6) and Tg-Nox4 (n = 6), $*p < 0.05$).

cooperatively with pericyte Nox4 after brain ischemia (unpublished data).

Nox4 expression is more strongly induced in peri-infarct areas after pMCAO than tMCAO

It is well known that oxidative stress is induced immediately after reperfusion following ischemia. Thus, it is thought to occur more strongly in tMCAO than pMCAO.[34] Unexpectedly, the upregulation of Nox4 was gradually induced and reached maximal levels at day 4 after brain ischemia, and was higher in pMCAO than in tMCAO (Figures 1b and c). Although there is a paper demonstrating the immediate upregulation of Nox4 after brain ischemia,[35] some papers have shown that Nox4 is significantly upregulated at 24 hours after MCAO in mice[36–38]. In particular, Kleinschnitz et al.[36] demonstrated the significant upregulation of Nox4 in the cortex at later than 24 hours after brain ischemia. Because brain infarcts were produced mainly in the cortex in our models, the time course of Nox4 upregulation in the present study is consistent with the previous reports. In addition, our in vitro study using cultured pericytes (Figure 3) may also support the time course of Nox4 upregulation in vivo after MCAO (Figure 1b). Since ROS can be produced from various enzymes other than Nox4 during ischemia/reperfusion,[39,40] Nox4 may not be a major enzyme responsible for ROS mediating oxidative and nitrative stresses immediately after ischemia/reperfusion.

NFκB phosphorylation and MMP-9 expression are significantly increased in pericytes overexpressing Nox4 both in vitro and in vivo

The phosphorylation of NFκB and production of MMP-9 were significantly increased in cultured pericytes overexpressing Nox4 (Figure 4) and in peri-infarct areas of Tg-Nox4 (Figure 5). ROS are key activators of NFκB.[41] Nox4 may be able to increase intracellular ROS leading to NFκB phosphorylation in pericytes.[42] Based on the present results, Nox4-mediated ROS may lead to the activation of IKK, which in turn induces the degradation of IκB and the subsequent stabilization and phosphorylation of NFκB[43] (Figure 4d and e), although further studies will be needed to elucidate how Nox4-mediated ROS induce IKK phosphorylation.

The close association between NFκB and MMP-9 has already been demonstrated.[7,44] It is thought that the expression and activity of two gelatinases, MMP-9 and MMP-2, are regulated differently: MMP-9, but not MMP-2, has NFκB binding sites in its promoter region and thus is upregulated by pro-inflammatory stimuli leading to the activation of NFκB.[44] The present results are well consistent with these facts.

BBB breakdown and MMP-9

BBB breakdown is a crucial determinant for enlargement of infarct volume after acute brain ischemia. Increased metalloproteinase activity of MMP-9 would degrade extracellular matrix proteins that are required for the maintenance of the BBB and the interaction between endothelial cells and pericytes, thereby leading to BBB breakdown.[30] MMP-9 is a major metalloproteinase in the brain after brain ischemia[30] and may be produced from various cell types, including pericytes.[7] It is known that MMP-9 activation and subsequent BBB breakdown occur biphasically after brain ischemia: blood cell-derived MMP-9 participates in the early breakdown of BBB within 1 day after stroke onset, while the delayed activation of MMP-9 is derived from components of the brain, including vascular cells, and may be involved in prolonged BBB breakdown at later than 1 day after stroke onset.[39,45] In addition, total MMP-9 activation appeared to be elicited more strongly in pMCAO than in tMCAO.[45] Collectively, Nox4 upregulated in microvascular pericyte could be an important component responsible for ROS leading to delayed/prolonged activation of MMP-9 and BBB breakdown after brain ischemia.

Is Nox4 good or bad in cardiovascular diseases?

We have demonstrated an adverse effect of pericyte Nox4 in acute brain ischemia. Consistent with the present study, Kleinschnitz et al.[36] have demonstrated that infarct volume, produced by either tMCAO or pMCAO, is significantly smaller with decreased oxidative stress, BBB breakdown, and apoptotic neuronal death in the mice with systemic deletion of Nox4 than in their littermate controls, although they did not elucidate the detailed underlying molecular mechanisms. In contrast, a couple of papers demonstrated that endothelial Nox4 promotes angiogenesis and functions beneficially in hindlimb ischemia and chronic load-induced cardiac stress.[17,18,22] We consider that Nox4 may be involved primarily in angiogenesis and subsequent healing processes through enhancement of metalloproteinase activity, such as MMP-9, at a delayed phase (= later than 24 hours) after tissue damage, including brain ischemia. However, Nox4 overexpression in pericytes could cause excessive and/or prolonged angiogenic responses with enhanced metalloproteinase activity, thereby leading to the enhancement of BBB breakdown and deterioration of brain infarct at a delayed phase after brain ischemia. Effects of Nox4 may vary in different cell types, organ/tissues, or types of injury.

Limitations

In the present study, we used mice with human Nox4 transgene with an SM22α promoter region to examine

the roles of pericyte Nox4 in acute brain ischemia. Since SM22α is a protein expressed in SMCs as well as pericytes, a suggestion would be to use Nox4 overexpressing mice using a promoter region of more pericyte-specific molecules. However, no pericyte-specific proteins have been identified so far.[3] We therefore demonstrated that protein expression of Nox4 was higher in cultured pericytes than in SMCs, and was much more strongly induced in microvascular pericytes than in SMCs in peri-infarct areas in both WT and Tg-Nox4 mice (Figures 1d, 2b and Supplementary Figure 3c). Thus, we consider that the Nox4 transgenic mice using a promoter of SM22α could be used to evaluate the effects of pericyte Nox4 in peri-infarct areas in acute brain ischemia. Nevertheless, further experiments using mice with pericyte-specific deletion of Nox4 may be needed to confirm the results of the present study.

Infarct volumes in this study may be somewhat smaller than expected. One of the reasons is we used a distal MCAO stroke model. In addition, it is reported that infarct volume is smaller in FVB/N than commonly used C57BL/6 in stroke models.[46] Thus, we may have to test the reproducibility of the present data in other mouse strains, including C57BL/6, in future studies. In this context, because neurological deficit was very mild in both WT and Tg-Nox4, it was difficult to show the difference of neurological severity between them by neurological scorings. Instead, we evaluated histological changes caused by pericyte-specific Nox4 overexpression extensively and focused on its mechanisms in this study.

Funding

The author(s) disclosed receipt of the following financial support for the research, authorship, and/or publication of this article: The work was supported in part by a Grant-in-Aid for Scientific Research (C) (25461134) (to JK), (C) (26461145) (to TA) and (C) (26462163) (to YW) and a Grant-in-Aid for Young Scientists (B) (26861169) (to KN) from the Ministry of Education, Culture, Sports, Science and Technology, Japan; a grant from SENSHIN Medical Research Foundation, Japan (to TA); a grant from MSD, Japan (to TA); grants from the Takeda Science Foundation, Japan (to TA and JK); and a grant from the Innovation Center for Medical Redox Navigation (to TA).

Acknowledgments

We are grateful to Hideko Noguchi (Kyushu University) and Naoko Kasahara (Hisayama Research Institute for Lifestyle Diseases) for their technical support.

Declaration of conflicting interests

The authors declared no potential conflicts of interest with respect to the research, authorship, and/or publication of this article.

Authors' contributions

AN and TA contributed to conception and design, acquisition, analysis and interpretation of data, and drafting the manuscript; JK, KA, MT, KN, and YW to acquisition, analysis and interpretation of data; KI, JS, and TK to interpretation of data, critical revision of the manuscript, and final approval.

Supplementary material

Supplementary material for this paper can be found at http://jcbfm.sagepub.com/content/by/supplemental-data

References

1. Abbott NJ. Blood-brain barrier structure and function and the challenges for CNS drug delivery. *J Inherit Metab Dis* 2013; 36: 437–449.
2. Iadecola C. Neurovascular regulation in the normal brain and in Alzheimer's disease. *Nat Rev Neurosci* 2004; 5: 347–360.
3. Armulik A, Genove G and Betsholtz C. Pericytes: developmental, physiological, and pathological perspectives, problems, and promises. *Dev Cell* 2011; 21: 193–215.
4. Shen J, Ishii Y, Xu G, et al. PDGFR-beta as a positive regulator of tissue repair in a mouse model of focal cerebral ischemia. *J Cereb Blood Flow Metab* 2012; 32: 353–367.
5. Fernandez-Klett F, Potas JR, Hilpert D, et al. Early loss of pericytes and perivascular stromal cell-induced scar formation after stroke. *J Cereb Blood Flow Metab* 2013; 33: 428–439.
6. Makihara N, Arimura K, Ago T, et al. Involvement of platelet-derived growth factor receptor beta in fibrosis through extracellular matrix protein production after ischemic stroke. *Exp Neurol* 2015; 264: 127–134.
7. Bell RD, Winkler EA, Singh I, et al. Apolipoprotein E controls cerebrovascular integrity via cyclophilin A. *Nature* 2012; 485: 512–516.
8. Zlokovic BV. Neurovascular pathways to neurodegeneration in Alzheimer's disease and other disorders. *Nat Rev Neurosci* 2011; 12: 723–738.
9. Balaban RS, Nemoto S and Finkel T. Mitochondria, oxidants, and aging. *Cell* 2005; 120: 483–495.
10. Bedard K and Krause KH. The NOX family of ROS-generating NADPH oxidases: physiology and pathophysiology. *Physiol Rev* 2007; 87: 245–313.
11. Sumimoto H. Structure, regulation and evolution of Nox-family NADPH oxidases that produce reactive oxygen species. *FEBS J* 2008; 275: 3249–3277.
12. Ago T, Kuroda J, Kamouchi M, et al. Pathophysiological roles of NADPH oxidase/nox family proteins in the vascular system. -Review and perspective. *Circ J* 2011; 75: 1791–1800.
13. Cave AC, Brewer AC, Narayanapanicker A, et al. NADPH oxidases in cardiovascular health and disease. *Antioxid Redox Signal* 2006; 8: 691–728.
14. Suh YA, Arnold RS, Lassegue B, et al. Cell transformation by the superoxide-generating oxidase Mox1. *Nature* 1999; 401: 79–82.

15. Lassegue B and Griendling KK. NADPH oxidases: functions and pathologies in the vasculature. *Arterioscler Thromb Vasc Biol* 2010; 30: 653–661.
16. Ago T, Kitazono T, Ooboshi H, et al. Nox4 as the major catalytic component of an endothelial NAD(P)H oxidase. *Circulation* 2004; 109: 227–233.
17. Craige SM, Chen K, Pei Y, et al. NADPH oxidase 4 promotes endothelial angiogenesis through endothelial nitric oxide synthase activation. *Circulation* 2011; 124: 731–740.
18. Schroder K, Zhang M, Benkhoff S, et al. Nox4 is a protective reactive oxygen species generating vascular NADPH oxidase. *Circ Res* 2012; 110: 1217–1225.
19. Hilenski LL, Clempus RE, Quinn MT, et al. Distinct subcellular localizations of Nox1 and Nox4 in vascular smooth muscle cells. *Arterioscler Thromb Vasc Biol* 2004; 24: 677–683.
20. Ago T, Kuroda J, Pain J, et al. Upregulation of Nox4 by hypertrophic stimuli promotes apoptosis and mitochondrial dysfunction in cardiac myocytes. *Circ Res* 2010; 106: 1253–1264.
21. Kuroda J, Ago T, Matsushima S, et al. NADPH oxidase 4 (Nox4) is a major source of oxidative stress in the failing heart. *Proc Natl Acad Sci U S A* 2010; 107: 15565–15570.
22. Zhang M, Brewer AC, Schroder K, et al. NADPH oxidase-4 mediates protection against chronic load-induced stress in mouse hearts by enhancing angiogenesis. *Proc Natl Acad Sci U S A* 2010; 107: 18121–18126.
23. Serrander L, Cartier L, Bedard K, et al. NOX4 activity is determined by mRNA levels and reveals a unique pattern of ROS generation. *Biochem J* 2007; 406: 105–114.
24. Nisimoto Y, Jackson HM, Ogawa H, et al. Constitutive NADPH-dependent electron transferase activity of the Nox4 dehydrogenase domain. *Biochemistry* 2010; 49: 2433–2442.
25. Taketo M, Schroeder AC, Mobraaten LE, et al. FVB/N: an inbred mouse strain preferable for transgenic analyses. *Proc Natl Acad Sci U S A* 1991; 88: 2065–2069.
26. Arimura K, Ago T, Kamouchi M, et al. PDGF receptor beta signaling in pericytes following ischemic brain injury. *Curr Neurovasc Res* 2012; 9: 1–.9.
27. Tokami H, Ago T, Sugimori H, et al. RANTES has a potential to play a neuroprotective role in an autocrine/paracrine manner after ischemic stroke. *Brain Res* 2013; 1517: 122–132.
28. Shichita T, Sugiyama Y, Ooboshi H, et al. Pivotal role of cerebral interleukin-17-producing gammadeltaT cells in the delayed phase of ischemic brain injury. *Nat Med* 2009; 15: 946–950.
29. Lin TN, He YY, Wu G, et al. Effect of brain edema on infarct volume in a focal cerebral ischemia model in rats. *Stroke* 1993; 24: 117–121.
30. Asahi M, Wang X, Mori T, et al. Effects of matrix metalloproteinase-9 gene knock-out on the proteolysis of blood-brain barrier and white matter components after cerebral ischemia. *J Neurosci* 2001; 21: 7724–7732.
31. Winkler EA, Bell RD and Zlokovic BV. Pericyte-specific expression of PDGF beta receptor in mouse models with normal and deficient PDGF beta receptor signaling. *Mol Neurodegener* 2010; 5: 32.
32. Kuroda J, Ago T, Nishimura A, et al. Nox4 is a major source of superoxide production in human brain pericytes. *J Vasc Res* 2014; 51: 429–438.
33. Vovenko E. Distribution of oxygen tension on the surface of arterioles, capillaries and venules of brain cortex and in tissue in normoxia: an experimental study on rats. *Pflugers Arch* 1999; 437: 617–623.
34. Kahles T and Brandes RP. Which NADPH oxidase isoform is relevant for ischemic stroke? The case for nox 2. *Antioxid Redox Signal* 2013; 18: 1400–1417.
35. Li H, Wang Y, Feng D, et al. Alterations in the time course of expression of the Nox family in the brain in a rat experimental cerebral ischemia and reperfusion model: effects of melatonin. *J Pineal Res* 2014; 57: 110–119.
36. Kleinschnitz C, Grund H, Wingler K, et al. Post-stroke inhibition of induced NADPH oxidase type 4 prevents oxidative stress and neurodegeneration. *PLoS Biol* 2010; 8: e1000479.
37. Wang Y, Jia J, Ao G, et al. Hydrogen sulfide protects blood-brain barrier integrity following cerebral ischemia. *J Neurochem* 2014; 129: 827–838.
38. Zhang HF, Li TB, Liu B, et al. Inhibition of myosin light chain kinase reduces NADPH oxidase-mediated oxidative injury in rat brain following cerebral ischemia/reperfusion. *Naunyn Schmiedebergs Arch Pharmacol* 2015; 388: 953–963.
39. Jickling GC, Liu D, Stamova B, et al. Hemorrhagic transformation after ischemic stroke in animals and humans. *J Cereb Blood Flow Metab* 2014; 34: 185–199.
40. Walder CE, Green SP, Darbonne WC, et al. Ischemic stroke injury is reduced in mice lacking a functional NADPH oxidase. *Stroke* 1997; 28: 2252–2258.
41. Clark RA and Valente AJ. Nuclear factor kappa B activation by NADPH oxidases. *Mech Ageing Dev* 2004; 125: 799–810.
42. Romeo G, Liu WH, Asnaghi V, et al. Activation of nuclear factor-kappaB induced by diabetes and high glucose regulates a proapoptotic program in retinal pericytes. *Diabetes* 2002; 51: 2241–2248.
43. Gloire G, Charlier E, Rahmouni S, et al. Restoration of SHIP-1 activity in human leukemic cells modifies NF-kappaB activation pathway and cellular survival upon oxidative stress. *Oncogene* 2006; 25: 5485–5494.
44. Yan C and Boyd DD. Regulation of matrix metalloproteinase gene expression. *J Cell Physiol* 2007; 211: 19–26.
45. Aoki T, Sumii T, Mori T, et al. Blood-brain barrier disruption and matrix metalloproteinase-9 expression during reperfusion injury: mechanical versus embolic focal ischemia in spontaneously hypertensive rats. *Stroke* 2002; 33: 2711–2717.
46. Carmichael ST. Rodent models of focal stroke: size, mechanism, and purpose. *NeuroRx* 2005; 2: 396–409.